Carbohydrate Polymers 117 (2015) 370–376

Contents lists available at ScienceDirect

Carbohydrate Polymers

journal homepage: www.elsevier.com/locate/carbpol

Chemical structure of the arabinogalactan protein from gum ghatti and its interaction with bovine serum albumin

Kanika Ghosh, Sayani Ray, Debjani Ghosh, Bimalendu Ray*

Natural Products Laboratory, Department of Chemistry, The University of Burdwan, Golapbag, Burdwan 713 104, West Bengal, India

ARTICLE INFO

Article history:
Received 24 June 2014
Received in revised form
14 September 2014
Accepted 22 September 2014
Available online 7 October 2014

Keywords:
Anogeissus latifolia gum
Arabinogalactan protein
Smith degradation
ESMS analysis
AGP–BSA interaction

ABSTRACT

Exudate gums, because of their beneficial properties, have been significant items of international trade in various industries for centuries. This manuscript sets out to gain insight into the fine structural details of an arabinogalactan protein (AGP) of gum ghatti (*Anogeissus latifolia* gum). The presence of a highly branched 554 kDa AGP having 1,6-linked Gal*p*, 1,2-linked Man*p*, 1,3-linked Ara*f* and 1,4-linked Glc*p*A main chain, substituted at *O*-4,6 of 1,2-linked Man*p*, and *O*-3/*O*-3,4 of 1,6-linked Gal*p* residues by Ara*f*, Ara*p* and Gal*p* units was revealed by chemical, chromatographic, ESMS, and NMR analyses. In particular, ESMS analysis of per acetylated oligomeric fragments derived from AGP by Smith degradation followed by acetylation was described as a commanding tool for providing critical structural information on a spectrum of glycerol tagged oligosaccharides. In addition, formation of an electrostatically driven complex between the isolated AGP and bovine serum albumin resulting in changes in the microenvironment around the tryptophan residues of BSA was established. A moderate radical scavenging activity comparable with those of standard antioxidants was observed from the AGP fraction (~94% at 1 mg/mL) that could be valuable in foods or pharmaceutical products as alternatives to synthetic antioxidants.

1. Introduction

For thousand of years exudates gums have been important articles of international trade in the food, pharmaceutical, adhesive, paper, textile, and other industries. Gum ghatti, the exudates from the large deciduous tree *Anogeissus latifolia* (*Combretacea*e, Myrtales), is one such item that have been widely evaluated in food and certain biotechnology industries (Deshmukh, Setty, Badiger, & Muralikrishna, 2012). The generally regarded as safe status of gum ghatti in USA is affirmed in 1976, but the EEC because of the lack of the more detailed safety evaluation deleted it from the European list of approved additives (Stephen & Churms, 1995). Renewed interest in gum ghatti is primarily due to its excellent emulsification properties (Castellani, Al-Assaf, Axelos, Phillips, & Anton, 2010a; Castellani et al., 2010b; Kaur, Singh, & Singh, 2009), which is probably better than gum Arabic (Ido et al., 2008). Moreover, the cost is attractive, comparable with that of gum Arabic. Also, the quality of this gum has been improved and its emulsification mechanism is clarified (Ido et al., 2008; Katayama et al., 2008). Indeed, the acceptance of gum ghatti in food in Japan, Latin America and other countries, have made it an alternative hydrocolloid for the food industry as a thickener and emulsifying agent (Castellani et al., 2010a).

Despite the well-recognized importance of the polysaccharide from gum ghatti and more than fifty years of investigation following their first description (Aspinall, Hirst, & Wickstrom, 1955), finer structural details are still missing. The complex nature of the molecular core and extreme size heterogeneity presents a major technical difficulty defying detailed structural analysis. To date, principal findings from two complementary analytical approaches essentially conceptualize and confine our current understanding of the polysaccharide from gum ghatti. First, chemical and chromatographic analyses of the oligosaccharides generated from gum ghatti has led to recognition of a molecular core comprising of alternating 1,4-linked β-D-Glc*p*A and 1,2-linked D-Man residues to which extremely complex arrays of neutral sugar units (Gal*p*, Ara*f*, and Ara*p*) and Glc*p*A are attached (Aspinall et al., 1955; Aspinall, Auret, & Hirst, 1958; Aspinall, Bhavanan, & Christen, 1965; Aspinall & Christen, 1965; Aspinall & McKenna, 1968; Aspinall, 1969). Technically, this chemical strategy was powerful but tedious. In contrast, using methylation analysis and NMR spectroscopy Kang and coworkers reported the presence of a highly branched polysaccharide containing 1,4-linked Glc*p*A, 1,6-linked Gal*p* and 1,2-linked L-Ara*f* main chain substituted at *O*-3 and *O*-4 of 1,6-linked β-D-Gal*p* residue by side chains (Kang et al., 2011a,b, 2012). A major

* Corresponding author. Tel.: +91 342 2557709; fax: +91 342 2564452.
E-mail addresses: bimalendu_ray@yahoo.co.uk, bimalendu.ray@gmail.com (B. Ray).

http://dx.doi.org/10.1016/j.carbpol.2014.09.084
0144-8617/

limitation though was to establish the sequence of sugar residues in the high molecular weight heteropolysaccharide particularly as it was not possible to assign even all anomeric signals. These seminal studies not only indicated some fundamental difference in the respective polysaccharide architecture but also gave rise to the different structural model.

Critical to gaining a better understanding at the structural level is the use of analytical tools that would allow mapping and sequencing of larger oligomeric motifs. We report here how Smith degradation have been effectively coupled to ESMS instrumentation to provide new structural insight of an arabinogalactan protein (AGP) isolated for the first time from gum ghatti, based on ESMS mapping and MS/MS sequencing of the released oligomeric fragments, after chemical acetylation. Further information on AGP structure was obtained by ESMS analysis of oligosaccharides generated by enzyme and acid hydrolysis. These results together with the data obtained from methylation analysis, NMR spectroscopy and size exclusion chromatography presented finer structural details into the AGP constituent of *A. latifolia* gum. Concerning technical aspects, the described procedure that helps to characterize oligmeric fragments derived from AGP by Smith degradation may similarly beneficial for the chemical characterization of polysaccharides of other sources.

Arabinogalactan-proteins (AGPs) are found in plasma membranes, cell walls, and plant exudates (Seifert & Roberts, 2007). Remarkably, both the intact AGPs and purified arabinogalactan of many plants possess immunomodulatory, hypoglycemic, and other biological activities, which are hot spots of research on functional factors of protective foods (McLean-Ross, Eastwood, Brydon, Busuttil, & McKay, 1983; Ozaki, Oki, Suzuki, & Kitamura, 2010). Although gum ghatti is consumed in daily food and beverage, there is no definite scientific evidence about its possible biological effects. So, we have evaluated the antioxidative activity of this polymer using the free radical scavenging capacity measurement.

Protein–carbohydrate interactions are critical for many biological systems, pharmaceutical products and processed food e.g., purification of macromolecules, microencapsulation of ingredients or cosmetics, fat substitutes, meat analogues, films, coatings, packaging, etc (Schmitt, Sanchez, Desobry-Banon, & Hardy, 1998; Dickinson, 2003). Consequently, it is important to define the structural bases for these macromolecular interactions. In addition, the development of protein/polyanion complexes retaining water solubility and stability over a wide pH range would enlarge their potential applications. Hence, the complex formation between bovine serum albumin (BSA), a transport protein and the arabinogalactan protein (AGP) of gum ghatti has been studied to elucidate the influence of pH, salt and concentration of AGP on complex formation. It is shown that water soluble stoichiometric BSA/AGP complexes are formed particularly when the protein molecules are positively charged, i.e., pH is lower than 4.7, while salt inhibits their formation. Remarkably, the UV–vis and fluorescence sprectroscopic techniques, which were used for the first time to study the electrostatically driven interaction between BSA and AGP, were found to be extremely useful.

2. Experimental

2.1. General experimental procedures

Dialysis (molecular cut-off 12 kDa; Sigma-Aldrich) against distilled H_2O were performed with continuous stirring. Evaporations were carried out with an Eyela N-1100 rotary evaporator under reduced pressure below 50 °C. Small volumes of sample solutions were freeze-dried with a ScanVac Cool Safe 55-F freeze drier. Moisture was determined by drying ground material in an oven at 110 °C for 3 h. Total carbohydrate content was estimated by the phenol–sulfuric acid assay using galactose/arabinose = 1/1 (wt/wt) as standard (Dubois, Gilles, Hamilton, Rebers, & Smith, 1956). Total uronic acid was assayed as anhydrogluronic acid by *m*-hydroxydiphenyl color reagent using GlcA as standard (Ahmed & Labavitch, 1977). For the determination of sugar composition, the monosaccharide residues released by acid hydrolysis were converted into their alditol acetates (Blakeney, Harris, Henry, & Bruce, 1983) and analyzed by GC and GC–MS. Monosaccharides were also identified by thin-layer chromatography using sulfosalicylic acid as the color developing reagent (Ray, Ghosal, Thakur, & Majumdar, 1984). Alternatively, TMS-derivatives of methyl glycosides were analyzed by GC (York, Darvill, O'Neill, Stevenson, & Albersheim, 1985). UV–vis spectra were recorded on a Shimadzu UV-2450 UV–vis spectrophotometer, and Fluorescence spectra were recorded on a Perkin Elmer precisely L-55 fluorescence spectrophotometer with an excitation wave length (λ_{ex}) of 282 nm, using 5 nm excitation and 6.5 nm emission slit widths. The NMR spectra (HSQC, NOESY, COSY-Relay, ^{1}H- and ^{13}C-NMR) were recorded on a Bruker DRX-500 NMR spectrometer at 25 °C in D_2O solvent. GC was carried out with a Shimadzu GC-17A chromatograph fitted with a flame ionization detector, and a DB-225 column (30 m × 0.53 mm i.d.), using a program that maintained an isocratic temperature of 210 °C for 18 min and helium as gas vector. GC–MS was performed with a Shimadzu QP 5050A GC–MS instrument at 70 eV. Conditions for GC–MS were as described previously (Majumder, Morvan, Thakur, & Ray, 2004).

Determination of molecular mass was performed by high performance size exclusion chromatography (HPSEC) using a multiangle laser light scattering (MALLS) setup (MiniDawn, Wyatt, Santa Barbara, CA) operating at three angles (41°, 90°, and 138°); universal calibration curve established with pullulans in the range 5–1600 × 10^3 g/mol), a UV detector, and a differential refractometer (RI; ERC 7547A). The refractive index increment (d*n*/d*c*) of gum ghatti determined experimentally was used and molecular weight was calculated using Astra 1.4 software (MALLS).

Protein content was measured by Bradford method using bovine serum albumin as standard. Amino acids were released by hydrolysis with 6 M HCl at 110 °C for 22 h in a sealed tube (Majumder et al., 2004). The liberated amino acids were analysed by Pharmacia LKB ALPHA PLUS amino acid analyser. Electrospray mass spectra (ESMS) and tandem mass spectra (ESMS/MS) were measured on a quadrupole instrument (Micromass Q-Tof micro™, Water Pvt. Ltd.). Samples were dissolved in CH_2Cl_2 or MeOH/H_2O = 1/1 and injected at flow rate 10.0–20.0 μL/min. The capillary voltage and the cone voltage were set at 3.0–3.1 kV and 30–60 V, respectively. The source capillary was at a temperature of 150–200 °C.

2.2. Plant material

The dried gum of *A. latifolia* trees (LOT-0000107081) was from Himedia Laboratories Pvt. Ltd. (Mumbai, India) and powdered before extraction.

2.3. Isolation and purification of the arabinogalactan protein (AGP)

The crushed material of gum ghatti (5 g) was treated with distilled water (3 × 0.5 L) at 120 °C under presser (100 kPa) for 1 h. After removing the insoluble residue by filtration through a glass filter (G2), the combined extract was evaporated to a small volume, and diluted with cold Me_2CO (×3 volumes). The precipitate was then dissolved in H_2O, and the resulting solution lyophilized to yield the water extracted carbohydrate polymer (CP, ~3.2 g). Anion exchange chromatography of a solution 10 mL (5 mg/mL) of CP in water (pH 6.5) on Amberlite IRA-400 (OH^-) (BDH Chemical)

column (2 × 16 cm) yielded a water eluted fraction (F1). In a separate experiment, this F1 fraction was re-chromatographed on the same column under similar experimental condition. AGP was isolated according to Schultz, Johnson, Currie, and Bacic (2000). Briefly, to a solution of F1 in 1% NaCl (w/w) was added an equal volume of Yariv reagent dissolved in 1% NaCl. The mixture was kept at 4–8 °C for 18 h and then centrifuged. The pellet was washed with 1% NaCl followed by pure methanol (three times each), dried and then treated with sodium metabisulfite (10%). The resulting solution was then dialyzed and freeze dried to yield the arabinogalactan protein (AGP).

2.4. Analytical methods

This material is available free of charge via the Internet at http://www.sciencedirect.com/.

3. Results and discussion

3.1. Chemical characterization of the antioxidative arabinogalactan protein

3.1.1. Isolation of an arabinogalactan protein (AGP)

An AGP containing fraction was isolated from *A. latifolia* gum by the following procedures: (1) extraction of the dried gum with water 120 °C, (2) precipitation by adding acetone (×3 volumes), and (3) purification by anion exchange chromatography. The water eluted fraction (F1) from the ion exchanger that corresponds to 66% (w/w) of CP had a molecular mass of 554,000 g/mol (Fig. S1 in Supplementary data) and it contained Ara, Gal, Man and GlcA in a molar ratio of 59/32/3/6. This high molecular mass compound contained 7% (w/w) protein. The major components were aspartic acid/asparagine (17.5%), lysine (9.5%), glutamic acid/glutamine (8.9%) and glycine (9.2%). The UV spectrum of F1 showed a strong absorbance band at about 205 nm and a weak absorbance band at about 277 nm, which further indicated that the existence of protein. Finally, ~94% of F1 was precipitated with the β-glucosyl Yariv reagent and hence marked as arabinogalactan protein (AGP).

3.1.2. Glycosidic linkage analysis suggests that the AGP is highly branched

The results of the glycosidic linkage analysis, as summarized in Table 1, revealed the presence of a highly branched structure, containing nonreducing end-units of Ara*f* (2,3,5-Me_3-Ara), Ara*p* (2,3,4-Me_3-Ara), and Gal*p* (2,3,4,6-Me_4-Gal). The galactopyranosyl units were, mainly, 1,6-, 1,3,6- and 1,3,4,6-linked, in accord with 2,3,4-Me_3-Gal; 2,4-Me_2-Gal and 2-Me_1-Gal methylated derivatives, respectively (Fig. S2 in Supplementary data). Small amount of 1,2- and 1,2,4,6-substituted mannopyranosyl units were present as demonstrated by the presence of 3,4,6-Me_3-Man and 3-Me_1-Man derivatives. The arabinosyl units were 1,2- and 1,3-linked Ara*f*, in accord with 3,5-Me_2-Ara, and 2,5-Me_2-Ara derivatives, respectively. Earlier data revealed that Glc*p*A residues were 1,4-linked (Aspinall et al., 1955, 1958, 1965; Aspinall & Christen, 1965; Aspinall & McKenna, 1968; Kang et al., 2011a,b, 2012; Tischer, Iacomini, Wagner, & Gorin, 2002), but the existence of large quantities of terminal residues compared to branch points indicated that a part of the GlcA units were probably substituted (Table 1).

Table 1
Glycocidic linkage analysis of AGP of *A. latifolia* and its Smith degraded derivatives (SD1P and SD1S).

Sugars and linkages	Peak area[a]		
	AGP	SD1S	SD1P
Arabinose			
Terminal-Ara*f*	51	24	5
2-Ara*f*	4		
3-Ara*f*	4	2	14
Terminal-Ara*p*	1		
Galactose			
Terminal-Gal*p*	1	26	1
1,6-Gal*p*	10	48	73
1,3,6-Gal*p*	10		
1,3,4,6-Gal*p*	16		
Mannose			
1,2-Man*p*	1		5
1,2,4,6-Man*p*	2		
1,2,4-Man*p*			2

[a] Percentage of total area of the identified peaks.

3.1.3. Smith degradation in conjunction with mass spectrometry provided further insights of AGP structure

Smith degradation of AGP produced an ethanol soluble oligomeric fraction (SD1S) containing Ara attributable to T-/1,3-linked Ara*f* residues, as well as Gal assigned to T-/1,6-linked Gal*p* residues (Table 1). On the other hand, the ethanol precipitated polymeric fraction (SD1P) was made up of Gal, Ara, Man and GlcA in molar ratio of 60/15/6/19. The protein content (11%) of this fraction was higher than that of parental AGP in agreement with the destruction of many monosaccharide units by IO_4^- oxidation. Indeed, most (96%) of the Ara and majority (65%) of GlcA units were eliminated during Smith degradation. Intriguingly, the survival of GlcA during IO_4^- oxidation confirmed that at least a part of the total GlcA units in AGP are substituted. Notably, in accord with 74 mM of IO_4^- was consumed by 100 mM sugar units. As the molecular mass of SD1P, which contained 11% protein, is 15 kDa (Fig. S1 in Supplementary data) this oxidised polymeric fraction contained approximately 77 monosaccharide units. Regarding glycosidic linkage pattern, the Gal*p* units in SD1P were either terminal or 1,6-linked (Fig. S2 in Supplementary data). It also contained terminal and 1,3-linked Ara*f*, in accord with 2,3,5-Me_3-Ara, and 2,5-Me_2-Ara derivatives, respectively. This result is contrast that of Kang et al. (2011a,b, 2012) where the presence of 1,2-linked Ara residues in the backbone was inferred. Second Smith degradation of SD1P yielded a product (SD2) containing mostly protein together with only a trace of Man units suggesting that the protein part were probably linked to the polysaccharides via Man residues.

Changes in structure between the AGP and its Smith degraded derivative (SD1P) were also evident from their ^{1}H NMR spectra (Fig. 1). For example, the anomeric signals of Ara units were radically reduced by this chemical degradation in accord with the reduction of the T-Ara content of the polymer by periodic acid mediated cleaves of vicinal hydroxyl groups. Remarkably, H1 resonances of 1,6-, 1,3,6- and 1,3,4,6-linked Gal*p* residues, as shown in these spectra, appeared in the same region (Fig. S3–S5 in Supplementary data). Finally, NOESY experiment was used to determine the inter residual connectivity between sugar residues. Thus, T-Ara*f* residues in SD1P were linked to Glc*p*A through 1,2-*O*-glycosidic bond in accord with the presence of cross-peak between *H*-1 (5.24 ppm) of T-Ara*f* and *H*-2 (3.38 ppm) of 1,4-linked Glc*p*A residues (Fig. S5 in Supplementary data). The signals in the NMR spectrum were assigned according to sugar composition, glycosidic linkage makeup, 2D NMR techniques and data in the literature (Ghosh et al., 2013; Kang et al., 2011a,b, 2012; Samuelsen et al., 2007; Sims & Furneaux, 2003). Taken together, the molecular core of the AGP contained, *inter alia*, 1,3-linked Ara*f*, 1,4-linked Glc*p*A and 1,6-linked Gal*p* units. Glc*p*A units were substituted at *O*-2, whereas the Gal*p* residues at *O*-3 or *O*-3,4.

The oligomeric fragments (SD1S) generated by Smith degradation (Scheme 1) were analysed by ESMS after chemical acetylation. The peracetylated moities (SDAc) afforded a spectrum of better quality in comparison with that of native sample (not shown)

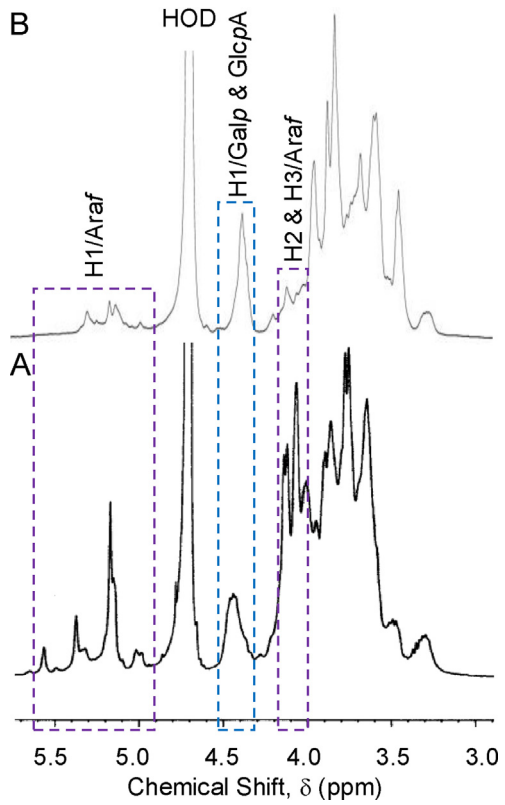

Fig. 1. Comparison of the ^{1}H NMR spectra of (A) the arabinogalactan protein of *A. latifolia* gum and (B) its Smith degraded derivative (SD1P).

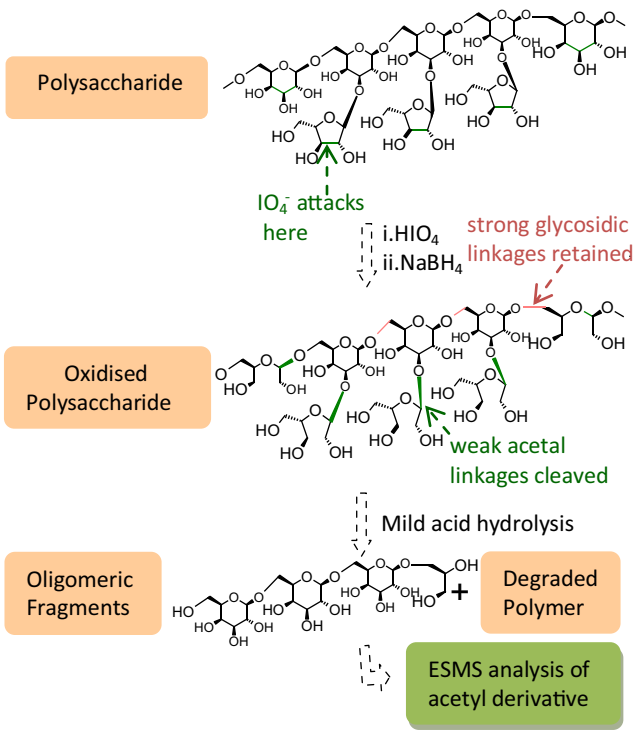

Scheme 1. Generation of a trisaccharide with glycerol tag at the reducing end by Smith degradation of the AGP fraction from *A. latifolia* gum.

and yielded only $[M+Na]^+$ molecular adduct (Table S1 in Supplementary data). As shown in Fig. 2 SDAc comprises four series of oligomeric signals each containing a glycerol label (*O*-Gly). The existence of only *O*-Gly tag at the reducing end of the generated oligomeric fragments was not surprising as 1,6-linked Gal unit upon Smith degradation produced *O*-Gly label (Scheme 1). On the other hand, the glycolic acetals generated by IO_4^- oxidation were easily hydrolyzed and not detected. In addition, the 1,3-linked Ara*f* and 1,3,6-/1,3,4,6-linked Gal*p* residues remained and joined glycosidically to interior sugar units or modified sugars. Although not absolutely quantitative, it was obvious from the signal intensity that $Gal_nGly_1Ac_{(3n+2)+2}$ series, where $n=1$–8, constituted the major digestion product (Fig. 2A). According to the glycosidic linkage analysis Gal units in SD1S were either terminal or 1,6-linked. Consequently, the existence of eight consecutive 1,6-link Gal units each substituted at

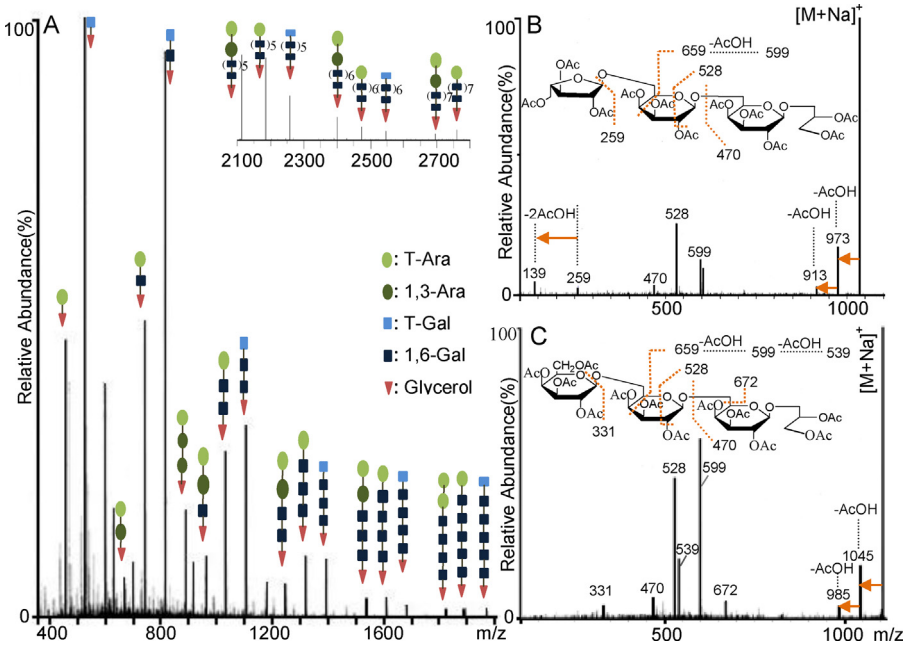

Fig. 2. Positive-ion ES mass spectrum of acetylated oligosaccharides with glycerol tag (SD-Ac) generated from AGP fraction of *A. latifolia* gum by Smith degradation. (A) Inset: expansion of *m*/*z* 2100–2800 region; MS/MS spectra of acetylated oligosaccharides with *m*/*z* at 1033 (B) and 1105 (C). Molecular ions are assigned as $[M+Na]^+$.

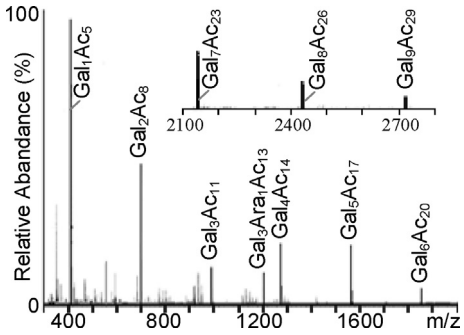

Fig. 3. ES mass spectrum of acetylated oligomeric fragments (AGPoseAc) generated from the AGP of *A. latifolia* gum by enzyme hydrolysis. Inset: expansion of *m*/*z* 2100–2700 region.

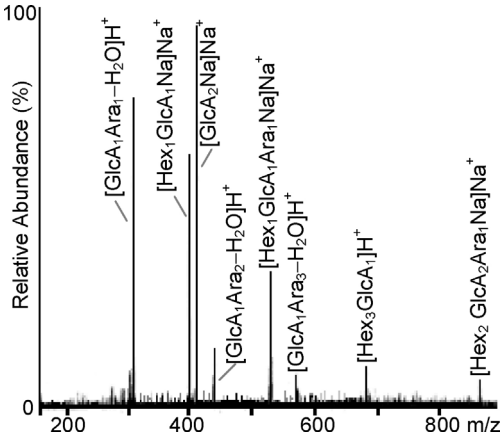

Fig. 4. ES mass spectrum of acidic oligosaccharides generated from the AGP of *A. latifolia* gum by partial acid hydrolysis.

either *O*-3 or *O*-3,6 in the parental AGP. The three other series were: $Ara_1Gal_nGly_1Ac_{(3n+2)+2+2}$ (n = 1–8), $Ara_2Gal_nGly_1Ac_{(3n+2)+2+4}$ (n = 1–7), and $Ara_nGly_1Ac_{(2n+2)+2}$ (n = 1–3). Arguably, the presence of first two series of oligosaccharides provided direct evidence for the existence of Ara and Gal units in the same molecule. The existence of three consecutive 1,3-linked Ara*f* were also revealed. Notably, fragments containing carboxylic acid groups were not detected by this method. To define the location of the arabinosyl residues in the generated oligomers, two molecular ions (*m*/*z* 1033 and 1105) afforded by the peracetyl derivatives were selected for collision induced dissociation (CID) ESMS/MS analysis (Fig. 2B–C). Notably, these spectra were characterized by intense fragments ions signals arised from sugar ring cleavages, in addition to weak signals due to glycosidic bond cleavages. The fragment ion at *m*/*z* 259 resulting from Ara residues of the 1033 parent ion (Fig. 2B), and the ion at *m*/*z* 470 suggested the presence of Ara–Gal–Gal–Gly as oligomeric subunit. Also one can see major ion structures as indicated by the intense signals at *m*/*z* 528 and 599. Incidentally, the presence of *O*-Gly label on the anomeric carbon of the reducing end makes the sequencing of Ara and Gal residues easier. Additionally, each of the $Gal_nGly_1Ac_{(3n+2)+2}$, where n = 1–8, oligomers detected in the spectra of the derivatives (Fig. 2) can be confidently ascribed to being present originally among the digestion products, and not derived from loss of Gal/Ara residues from larger oligomers during MS ionization. Thus, this approach constitutes a powerful tool for the characterization of moieties derived from polysaccharide by Smith degradation leading an important step forward for investigating the finer structural details of complex carbohydrates.

3.1.4. The enzyme and arabinogalactan protein of A. latifolia gum

The oligosaccharides (AGPose) generated from AGP by enzyme hydrolysis was analyzed by ESMS, after chemical acetylation (AGPoseAc). Remarkably, the enzyme-digestion profile (Fig. 3) comprised mainly of signals containing 1–8 Gal units (Table S2 in Supplementary data), indicating for the first time, the presence of galactose containing block. The intensity of signals of oligomers containing both Ara and Gal units was low. However, it is hardly surprising that, while some structural information has been gained by the use of specific enzymes to catalyze hydrolysis of certain bonds in some plant gums (Stephen & Churms, 1995), the complex nature of polysaccharide structures revolts against their being degraded in this way. Indeed, the function of gums in protecting the plant against microbial or fungal attack requires this type of resistance.

3.1.5. Partial acid hydrolysis

The acidic oligomers (AO) generated from AGP by partial acid hydrolysis were purified by anion exchange chromatography and then analyzed by ESMS without derivatization (Table S3 in Supplementary data). As highlighted in Fig. 4, AO contained several signals of oligosaccharides each containing at least one GlcA residue. The existence of $GlcA_1Ara_1$ and $GlcA_1Ara_2$ provided for the first time direct evidence for the linkage between Ara and GlcA residues. Notably, NOESY experiment revealed that α-L-Ara*f* residue was linked with 1,4-linked β-Glc*p*A residue by an 1,2-*O* glycosidic bond (Fig. S5 in Supplementary data).

3.1.6. Antioxidative property of the arabinogalactan protein

AGP exhibited a dose dependent DPPH radical scavenging activity over the concentration range 0.002–1.5 mg/mL (Fig. S6 in Supplementary data). Interestingly, the hydroxyl radical scavenging activity of this AGP gets closer to that of commercial antioxidants.

3.2. Formation of BSA-arabinogalactan protein complex is driven by electrostatic interaction

3.2.1. Polysaccharide binding assessed by UV spectroscopy

The UV–vis spectra of BSA in the presence of various concentration of AGP (0.36–3.61 μM) were indicated in Fig. 5A at pH 7.4. Without AGP, the absorption spectrum of BSA showed a strong peak centred on about 227 nm and another weaker peak centred near on 277 nm. The peak in the 227 nm region in the difference spectrum of proteins is related to changes in peptide backbone conformation; while the 277 nm peak represent changes in the environment of the tryptophan and tyrosine residues (Glazer & Smith, 1961). With gradual addition of AGP, the absorbance of peak at 227 nm decreased, shifted to longer wavelength (235 nm) and narrowed. These spectral changes arise from the disturbance of the microenvironment around the polypeptide backbone conformation caused by the binding of AGP with BSA. Such complex formation, which occurred above the pI of BSA (pI = 4.7) may be attributed to the attachment of negatively charged groups on the polysaccharide to positive patches on the surface of the BSA. A similar kind of behaviour was also observed when proteins and anionic polysaccharides were mixed together in aqueous solutions (Kruif, Weinbreck, & de Vries, 2004; Park, Muhoberac, Dubin, & Xia, 1992).

3.2.1.1. Effect of pH. Information about the influence of the pH on complex formation between AGP and BSA was obtained by UV measurements in the pH range of 4.0–10.0 (Fig. 5A–C). As illustrated in Fig. 5B, the UV–vis spectra of BSA at pH 4.0 showed significant change on both absorption peaks at 227 and 277 nm with gradual addition of the AGP to BSA solution. In particular, a significant increase in absorbance at 277 nm for BSA was observed, which was

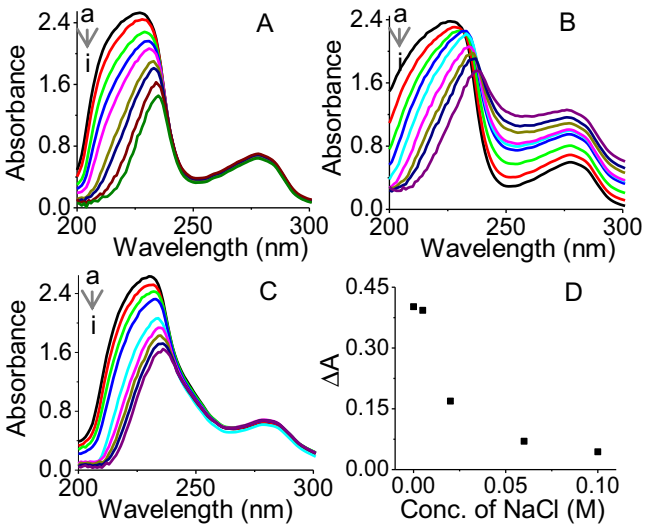

Fig. 5. Effect of AGP of *A. latifolia* on UV absorption of BSA at 25 °C in 100 mM phosphate buffer: (A) pH 7.4, (B) pH 4.0 and (C) pH 10.0. The black line (a) is the spectrum of native BSA (15 μM). The colored lines correspond to the spectra of BSA in the presence of 0.36, 0.72, 1.08, 1.80, 2.53, 2.89, 3.25, 3.61 μM AGP (*b–i*). (D) Difference in absorbance (ΔA) at 277 nm between 15 μM free BSA and in presence of 1.80 μM AGP at pH 4.0 in 100 mM phosphate buffer plot with various concentration of NaCl. (For interpretation of the references to color in this figure legend, the reader is referred to the web version of this article.)

indicative of a system containing complexes. Thus, addition of AGP modified environment around the aromatic amino acid residues. Remarkably, the extent of these tertiary structure changed due to complexation by AGP varies with concentration. The AGP–BSA binding constant, as determined using Hildebrand–Benesi equation using 15 μM BSA in presence of 0.36–3.61 μM AGP at 277 nm, was found to be $4.05 \times 10^5\ M^{-1}$. At pH 4.0, BSA carries a net positive charge, whereas AGP is negatively charged. Therefore, the driving force for complex formation is probably the electrostatic attraction between anionic polysaccharide molecule and cationic protein. Notably, at pH higher than 4.0 the obtained difference in absobance (ΔA) around 277 nm of BSA, i.e., ΔA values are close to zero, indicating that no important changes in the aromatic amino acid containing regions of BSA occurs.

3.2.1.2. Effect of salt. The influence of ionic strength was studied by adding various amount of salt (NaCl) to a mixture of AGP/BSA (molar ratio 3/25) at pH 4.0. Fig. 5D highlighted the strong effect of salt concentration on complex formation, since the addition of NaCl caused a significant decrease of the ΔA of BSA in presence of AGP to lower values below and above a critical [NaCl], complex formation was suppressed as was observed for their system by Weinbreck, de Vries, Schrooyen, and de Kruif (2003). The most likely reason for this effect was that as the ionic strength increased, the electrostatic repulsion between the polymers was progressively screened by the counter ions (Na^+ or Cl^-) surrounding the macromolecules, hence the magnitude of the electrostatic repulsion was reduced (Overbeek & Voorn, 1957; Schmitt et al., 1998). Thus, formation of complex coerced by electrostatic force was confirmed. Therefore, UV–vis spectroscopy is a powerful technique for studying the molecular interaction between arabinogalactan protein and bovine serum albumin. This procedure has the potency to provide critical information on the nature of interaction involved.

3.2.2. Fluorescence quenching measurement

The formation of complex between AGP and BSA was further confirmed by fluorescence quenching measurement. As shown in Fig. 6 the intrinsic fluorescence emission spectra for BSA in

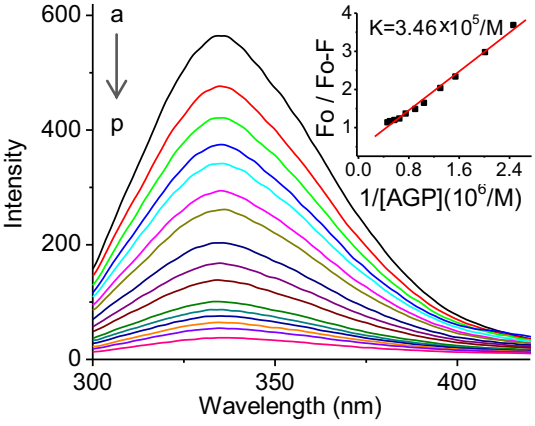

Fig. 6. Fluorescence emission spectra of BSA alone and in the presence of AGP at excitation wavelength of 282 nm in 100 mM phosphate buffer at pH 4.0: a: 0.75 μM BSA alone; *b–p*: 0.75 μM BSA with 0.18, 0.29, 0.41, 0.49, 0.65, 0.77, 0.96, 1.11, 1.33, 1.54, 1.76, 2.01, 2.19, 2.37, 2.55 μM AGP. Inset: plot of $F_0/(F_0 - F)$ as a function of [AGP]. The binding constant *K*, the ratio of intercept to slope, was obtained from modified Stern–Volmer equation.

the presence of increasing concentrations of AGP (0.04–24.30 μM) showed a concentration dependent decrease in intensity. The AGP absorbed a negligible amount of the 282 nm excitation light used and fluoresced around 334 nm. Consequently, the observed fluorescence quenching was due to the complexation of AGP with BSA. There are two Trp in BSA at positions 134 and 212 located in sub domains IB and IIA (Peters, 1985). Trp-134 is thought to be more solvent-exposed than Trp-212 as the former is located on the surface of the BSA molecule. Thus, it is likely that this quenching is due to Trp-134 residues, which are more accessible to quencher AGP ($M_{av} \sim 554$ kDa) compared to Trp-212. The quenching constant can be taken as the binding constant of the complexation reaction between fluorophore and quencher. The binding constant for AGP–BSA complexation was found to be $K = 3.46 \times 10^5$. Thus, the formation of water-soluble complex between BSA and AGP was revealed.

4. Conclusions

The findings of this study emphasized several unique and significant aspects of the *A. latifolia* gum derived AGP with regard to its structure and interaction with BSA: (i) the existence of blocks containing up to eight consecutive 1,6-linked Gal*p* residues substituted at *O*-3 and *O*-3,4 was established; (ii) the presence of only galactose containing block was exposed; (iii) the occurrence of at least three consecutive 1,3-linked Ara*f* residues was revealed; (iv) the existence of a periodate resistant block containing 77 monomeric units was indicated; (v) the studied macromolecule showed dose dependent antioxidative property; (vi) formation of electrostatically driven complex between AGP and BSA was suggested; and (vii) proof indicating changes in the microenvironment around the Trp residue of BSA was obtained. Concerning methodological aspects, fluorimetric and ultraviolet spectrometric procedures that have, for the first time, been used in this study may similarly be beneficial to study the interaction between BSA and AGPs of other gum polysaccharide. In addition, a novel strategy based on ESMS analysis of peracetylated oligomeric fragments generated by Smith degradation was developed. Not only molecular species can be characterised in this strategy but, also, subunits which are generated by collision between the ion source and the analyzer. This commanding technique that provided further insight into finer structural details of *A. latifolia* AGP may provide opportunities for the analysis of other complex carbohydrates.

Acknowledgements

Financial support from Department of Science and Technology (Grant number SR/S1/OC-38/2012), New Delhi, India, to B.R. is gratefully acknowledged.

Appendix A. Supplementary data

Supplementary data associated with this article can be found, in the online version, at http://dx.doi.org/10.1016/j.carbpol.2014.09.084.

References

Ahmed, A., & Labavitch, J. M. (1977). A simplified method for accurate determination of cell wall uronide content. *Journal of Food Biochemistry*, *1*, 361–365.
Aspinall, G. O., Hirst, E. L., & Wickstrom, A. (1955). Combreturn leonense gum. Part I. Partial hydrolysis of the gum. *Journal of Chemical Society*, 1160–1165.
Aspinall, G. O., Auret, B. J., & Hirst, E. L. (1958). Gum ghatti (Indian gum). Part III. Neutral oligosaccharides formed on partial acid hydrolysis of the gum. *Journal of Chemical Society*, 4408–4418.
Aspinall, G. O., Bhavanan, V. P., & Christen, T. B. (1965). Gum ghatti (Indian gum). Part V. Degradation of the periodate-oxidised gum. *Journal of Chemical Society*, 2673–2676.
Aspinall, G. O., & Christen, T. B. (1965). Gum ghatti (Indian gum). Part IV. Acidic oligosaccharides from the gum. *Journal of Chemical Society*, 2677–2684.
Aspinall, G. O., & McKenna, J. P. (1968). Araucaria bidwillii gum: Part II. Further studies on the polysaccharide components. *Carbohydrate Research*, *7*, 244–254.
Aspinall, G. O. (1969). Gums and mucilages. *Advances in Carbohydrate Chemistry and Biochemistry*, *24*, 333–379.
Blakeney, A. B., Harris, P., Henry, R. J., & Bruce, A. B. (1983). A simple rapid preparation of alditol acetates for monosaccharide analysis. *Carbohydrate Research*, *113*, 291–299.
Castellani, O., Al-Assaf, S., Axelos, M., Phillips, G. O., & Anton, M. (2010). Hydrocolloids with emulsifying capacity. Part 2—Adsorption properties at the *n*-hexadecane–water interface. *Food Hydrocolloids*, *24*, 121–130.
Castellani, O., Gaillard, C., Vie, V., Al-Assaf, S., Axelos, M., & Phillips, G. O. (2010). Hydrocolloids with emulsifying capacity. Part 3—Adsorption and structural properties at the air–water surface. *Food Hydrocolloids*, *24*, 131–141.
de Kruif, C. G., Weinbreck, F., & de Vries, R. (2004). Complex coacervation of proteins and anionic polysaccharides. *Current Opinion in Colloid and Interface Science*, *9*, 340–349.
Deshmukh, A. S., Setty, C. M., Badiger, A. M., & Muralikrishna, K. S. (2012). Gum ghatti: A promising polysaccharide for pharmaceutical applications. *Carbohydrate Polymers*, *87*, 980–986.
Dickinson, E. (2003). Hydrocolloids at interfaces and the influence on the properties of dispersed systems. *Food Hydrocolloids*, *17*, 25–39.
Dubois, M., Gilles, K. A., Hamilton, J. K., Rebers, P. A., & Smith, F. (1956). Colorimetric method for determination of sugars and related substances. *Analytical Chemistry*, *28*, 350–356.
Ghosh, D., Ray, S., Ghosh, K., Micard, V., Chatterjee, U. R., Ghosal, P. K., et al. (2013). Antioxidative carbohydrate polymer from *Enhydra fluctuans* and its interaction with bovine serum albumin. *Biomacromolecules*, *14*, 1761–1768.
Glazer, A. N., & Smith, E. L. (1961). Studies on the ultraviolet difference spectra of proteins and polypeptides. *Journal of Biological Chemistry*, *236*, 2942–2947.
Ido, T., Ogasawara, T., Katayama, T., Sasaki, Y., Al-Assaf, S., & Phillips, G. O. (2008). Emulsification property of GATIFOLIA (gum ghatti) used for emulsions in food products. *Foods and Food Ingredients Journal of Japan*, *213*, 365–372.
Katayama, T., Ido, T., Sasaki, Y., Ogasawara, T., Al-Assaf, S., & Phillips, G. O. (2008). Characterization of the adsorbed component of gum ghatti responsible for its oil–water interface advantages. *Foods and Food Ingredients Journal of Japan*, *213*, 372–376.
Kang, J., Cui, S. W., Phillips, G. O., Chen, J., Guo, Q., & Wang, Q. (2011a). New studies on gum ghatti (*Anogeissus latifolia*) Part II. Structure characterization of an arabinogalactan from the gum by 1D, 2D NMR spectroscopy and methylation analysis. *Food Hydrocolloids*, *25*, 1991–1998.
Kang, J., Cui, S. W., Phillips, G. O., Chen, J., Guo, Q., & Wang, Q. (2011b). New studies on gum ghatti (*Anogeissus latifolia*) Part III: Structure characterization of a globular polysaccharide fraction by 1D, 2D NMR spectroscopy and methylation analysis. *Food Hydrocolloids*, *25*, 1999–2007.
Kang, J., Cui, S. W., Guo, Q., Chen, J., Wang, Q., Phillips, G. O., et al. (2012). Structural investigation of a glycoprotein from gum ghatti. *Carbohydrate Polymers*, *89*, 749–758.
Kaur, L., Singh, J., & Singh, H. (2009). Characterization of gum ghatti (*Anogeissus latifolia*): A structural and rheological approach. *Journal of Food Science*, *74*, 328–332.
Majumder, S., Morvan, C., Thakur, S., & Ray, B. (2004). Cell wall polysaccharides from chalkumra (*Benincasa hispida*) fruit. Part I. Isolation and characterization of pectins. *Journal of Agricultural and Food Chemistry*, *52*, 3556–3562.
McLean-Ross, A. H., Eastwood, M. A., Brydon, W. G., Busuttil, A., & McKay, L. F. (1983). A study of the effects of dietary gum Arabic in humans. *The American Journal of Clinical Nutrition*, *37*, 368–375.
Overbeek, J. T. G., & Voorn, M. J. (1957). Phase separation in polyelectrolyte solutions. Theory of complex coacervation. *Journal of Comparative Physiology A: Sensory, Neural, and Behavioral Physiology*, *49*, 7–26.
Ozaki, S., Oki, N., Suzuki, S., & Kitamura, S. (2010). Structural characterization and hypoglycemic effects of arabinogalactan-protein from the tuberous cortex of the white-skinned sweet potato (*Ipomoea batatas* L.). *Journal of Agricultural and Food Chemistry*, *58*, 11593–11599.
Park, J. M., Muhoberac, B. B., Dubin, P. L., & Xia, J. (1992). Effect of protein charge heterogeneity in protein–polyelectrolyte complexation. *Macromolecules*, *25*, 290–295.
Peters, T., Jr. (1985). Serum albumin. *Advances in Protein Chemistry*, *37*, 161–245.
Ray, B., Ghosal, P., Thakur, S., & Majumdar, S. G. (1984). Sulphosalicylic acid as spray reagent for the detection of sugars on t.l.c. plate. *Journal of Chromatography*, *315*, 401–403.
Samuelsen, A. B., Westereng, B., Yousif, O., Holtekjølen, A. K., Michaelsen, T. E., & Knutsen, S. H. (2007). Structural features and complement-fixing activity of pectin from three *Brassica oleracea* varieties: White cabbage, kale, and red kale. *Biomacromolecules*, *8*, 644–649.
Schultz, C. J., Johnson, K. L., Currie, G., & Bacic, A. (2000). The classical arabinogalactan protein gene family of arabidopsis. *The Plant Cell*, *12*, 1751–1767.
Schmitt, C., Sanchez, C., Desobry-Banon, S., & Hardy, J. (1998). Structure and technofunctional properties of protein-polysaccharide complexes: A review. *Critical Reviews in Food Science and Nutrition*, *38*, 689–753.
Seifert, G. J., & Roberts, K. (2007). The biology of arabinogalactan proteins. *Annual Review of Plant Biology*, *58*, 137–161.
Sims, I. M., & Furneaux, R. H. (2003). Structure of the exudate gum from *Meryta sinclairii*. *Carbohydrate Polymers*, *52*, 423–431.
Stephen, A. M., & Churms, S. C. (1995). Gums and mucilages. In A. M. Stephen (Ed.), *Food polysaccharides and their applications* (pp. 441–462). New York, NY: Marcel Dekker Inc.
Tischer, C. A., Iacomini, M., Wagner, R., & Gorin, P. A. (2002). New structural features of the polysaccharide from gum ghatti (*Anogeissus latifola*). *Carbohydrate Research*, *337*, 2205–2210.
Weinbreck, F., de Vries, R., Schrooyen, P., & de Kruif, C. G. (2003). Complex coacervation of whey proteins and gum Arabic. *Biomacromolecules*, *4*, 293–303.
York, W. S., Darvill, A., O'Neill, M., Stevenson, T., & Albersheim, P. (1985). Isolation and characterization of plant cell walls and cell wall components. *Methods in Enzymology*, *118*, 3–40.